The Journal of Experimental Biology 214, 3880-3886

doi:10.1242/jeb.059808

RESEARCH ARTICLE

Ultrasound biomicroscopy for biomechanical characterization of healthy and injured triceps surae of rats

C. C. Peixinho[1,2,*], M. B. Ribeiro[3], C. M. C. Resende[4], J. P. S. Werneck-de-Castro[3], L. F. de Oliveira[2] and J. C. Machado[1,5]

[1]Biomedical Engineering Program, COPPE, Federal University of Rio de Janeiro, Rio de Janeiro, RJ, Brazil, [2]Laboratory of Biomechanics, Department of Biosciences and Physical Activity, Federal University of Rio de Janeiro, Rio de Janeiro, RJ, Brazil, [3]Laboratory of Exercise Biology, Department of Biosciences and Physical Activity, Federal University of Rio de Janeiro, Rio de Janeiro, RJ, Brazil, [4]Department of Radiology, School of Medicine, Clementino Fraga Filho University Hospital, Federal University of Rio de Janeiro, Rio de Janeiro, RJ, Brazil and [5]Post-Graduation Program in Surgical Sciences, Department of Surgery, School of Medicine, Federal University of Rio de Janeiro, Rio de Janeiro, RJ, Brazil

*Author for correspondence (carolina@peb.ufrj.br)

Accepted 28 July 2011

SUMMARY

This work describes the use of ultrasound biomicroscopy (UBM) to follow up the degeneration–regeneration process after a laceration injury induced in the lateral gastrocnemius (LG) and soleus (SOL) muscles of rats. UBM (40 MHz) images were acquired and used for biomechanical characterization of muscular tissue, specifically using pennation angle (PA) and muscle thickness (MT). The animals were distributed in three groups: the variability group (VG; *N*=5), the gastrocnemius injured group (GG; *N*=6) and the soleus injured group (SG; *N*=5). VG rats were used to assess data variability and reliability (coefficients of variation of 9.37 and 3.97% for PA and MT, respectively). GG and SG rats were submitted to the injury protocol in the LG and SOL muscles of the right legs, respectively. UBM images of muscles of both legs were acquired at the following time points: before and after injury (immediately, 7, 14, 21 and 28 days). We observed an increase in PA for the non-injured leg 28 days after injury for both GG and SG rats (GG=10.68 to 16.53 deg and SG=9.65 to 14.06 deg; *P*<0.05). Additionally, MT presented a tendency to increase (GG=2.92 to 3.13 mm and SG=2.12 to 2.35 mm). Injured legs maintained pre-injury PA and MT values. It is suggested that a compensatory hypertrophic response due to the overload condition imposed to healthy leg. The results indicate that UBM allows qualitative and quantitative muscle differentiation among healthy and injured muscle at different stages after lesion.

Key words: ultrasound biomicroscopy, muscle architecture, muscle injury.

INTRODUCTION

Ultrasound biomicroscopy (UBM) is a high-resolution imaging technique widely used in many areas of medicine and biology, mainly for detection, follow-up and diagnosis of diseases and injuries in humans and animals. It provides information without the need for biopsy and allows longitudinal studies *in vivo*. The UBM frequencies used in most applications vary from 40 to 60 MHz, corresponding to a resolution on the order of micrometers. That range of frequencies allows the generation of images of muscular tissue of small animals similar to those acquired with conventional ultrasound for humans (Megliola et al., 2006; Jacobson, 1999; Hashimoto et al., 1999).

Muscle architecture refers to structural characteristics of the muscle, including its fascicles (Blazevich, 2006; Koryak, 2008; Lieber and Bodine-Fowler, 1993), such as the pennation angle (PA), with respect to the axis of force generation, fiber length, muscle thickness (MT) and physiological cross-sectional area. Functional demands on skeletal muscle lead to a rearrangement of the muscle architecture, reflecting the maximum muscle force and contraction velocity. Therefore, the estimation of muscle architectural properties is highly justified as it provides the means to analyze muscle function.

Human muscle architecture data are available from cadaver studies (Wickiewicz et al., 1983; Ward et al., 2009). Concerning *in vivo* studies, imaging techniques, such as magnetic resonance and ultrasound, can monitor geometric changes within the muscle, i.e. fascicle length and angle changes (Narici, 1999; Kawakami et al., 1998; Kawakami, 2005; Fukunaga et al., 1997). These studies have demonstrated changes of the muscle architecture due to joint angle and contraction condition (passive or active). Additionally, muscle plasticity, when submitted to different experimental models of increased use or disuse, is also reported in studies with humans (Blazevich, 2006; Blazevich et al., 2007; Boonyarom and Inui, 2006; Kawakami, 2005). However, the tracking of the muscle degeneration–regeneration process in humans with reliable methodologies and quantification of architectural parameters has not yet been carried out because of inherent ethical difficulties.

Regarding animal studies, there are data related to muscle architecture obtained *in vitro* for some species, including rats. Recently, Eng et al. (Eng et al., 2008) presented a study that examined muscle architecture and fiber type in the rat hindlimb to define the functional specialization of each muscle. Nevertheless, a literature search for studies quantifying skeletal muscle architectural parameters of rats *in vivo* was unsuccessful. Studies with animals related to the degeneration–regeneration process subsequent to muscle injury are restricted to *in vitro* analysis and do not permit longitudinal follow-up.

High-resolution images of skeletal muscle of rats can be useful to establish injury models and to track muscle adaptations through time. Other studies have already indicated the possibility of obtaining real-time *in vivo* skeletal muscle images of rats using high-resolution ultrasound. For instance, UBM has been used to study embryonic development through *in utero* images of small animals (Foster, 2003; Foster et al., 2002) and Witte et al. (Witte et al., 2004) used UBM to describe the coordination of individual fibers of a rat and a mouse through *ex vivo* tests.

The present study aims to evaluate the extension and severity of a laceration injury, and to follow up the regeneration process using an animal model from a biomechanical point of view. We employ the UBM technique to generate high-resolution images of lateral gastrocnemius (LG) and soleus (SOL) muscles of healthy and injured rats; these images are used to quantify two architectural parameters (PA and MT) at different intervals after injury. The UBM technique also evaluates the reliability of the digitizing procedures, including the choice of measurement sites, image acquisition, and digitization and calculation of architectural parameters. *In vivo* analysis adds differential relevant information to traditional *in vitro* results, as muscle function is evaluated under normal or common live physiological conditions, with preservation of neural, vascular and muscular components.

MATERIALS AND METHODS

UBM system

A UBM system (Vevo 770; VisualSonics, Toronto, Canada) with a center frequency of 40 MHz was used (Fig. 1). This instrument produces small angle sector images (almost rectangular) with a 10×10 mm field of view and a frame rate of 34 Hz. Lateral and axial resolution were 80 and 40 μm, respectively.

Animals

All experiments conformed to the relevant regulatory standards of care and use of experimental animals. Wistar female rats [*Rattus norvegicus* (Berkenhout 1769); 2–3 months, 214.8±12.3 g] were distributed in three groups: the variability group (VG; *N*=5), the soleus injury group (SG; *N*=5) and the lateral gastrocnemius injury group (GG; *N*=6).

VG animals were tested with the ankle randomly positioned in neutral and full extension (Fig. 2) to assess the reliability of digitizing procedures and the variability of the parameters that was due to ankle angle. Three of the animals were repeatedly assessed on two different days because of the loss of two animals by unknown causes. The neutral and full extension positions were defined previously based on the possibility of limb immobilization. The ankle angle was determined from pictures taken from the immobilized limb using a digital camera (Panasonic DMC-FX12; Matsushita Electric Industrial Co., Osaka, Japan).

SG and GG animals were subjected to a laceration injury protocol on the right limb and used to follow up the regeneration process. The injury protocol was applied immediately after acquisition of images of healthy muscles to obtain images at the following time points: healthy, immediately after, and 7, 14, 21 and 28 days after injury. All animals were killed 30 days after injury for histological analysis.

An additional group of five Wistar female rats (2–3 months, 283.4±27.9 g) was used as a control for the parameters of muscle architecture during a period of 28 days corresponding to the duration of the test for the other groups. The PA and MT of SOL and LG were measured in this group at 0, 7, 21 and 28 days post injury.

Experimental protocol of laceration injury

The laceration model, developed at the Biophysics Laboratory of the Federal University of Rio de Janeiro, is based in the model described by Menetrey et al. (Menetrey et al., 1999) and adapted to SOL and LG muscles. The restrained rats were anesthetized with an intraperitoneal injection of ketamine (10–15 mg kg^{-1}) and xylazine (50–75 mg kg^{-1}). Once deep anesthesia was induced, a posterior longitudinal skin incision was made at the calf area of the right limb, and a subcutaneous dissection was performed to permit open exposure of the LG or the SOL. LG muscles had their bellies cut at 60% of the length from their distal insertion, through 50% of their width and 50% of their thickness, whereas SOL muscles were cut at 60% of the length from their distal insertion at their lateral border, through 50% of their width and 100% of their thickness.

Image acquisition

Prior to image acquisition, the animals were anesthetized and had their right and left legs shaved to avoid interference in the image. Animals were positioned in ventral decubitus at the equipment platform and their ankle was randomly immobilized in neutral position (VG) and full extension (VG, GG and SG) with the posterior leg free to be assessed with the UBM probe, which was positioned longitudinally relative to the segment's axis. The UBM machine was always operated by the same individual. The images of the LG and the SOL were obtained with the muscle positioned in the depth of field of the ultrasound beam; those images with sufficient fiber distinction or with clear visualization of the site of injury were saved for further analysis. The experimental setup of the test is shown in Fig. 1.

The probe was coated with ultrasound gel to aid acoustic coupling and avoid contact between the probe and the skin. Thus, minimal pressure was applied to the muscle in order to avoid interferences in MT and fascicle angle measurements.

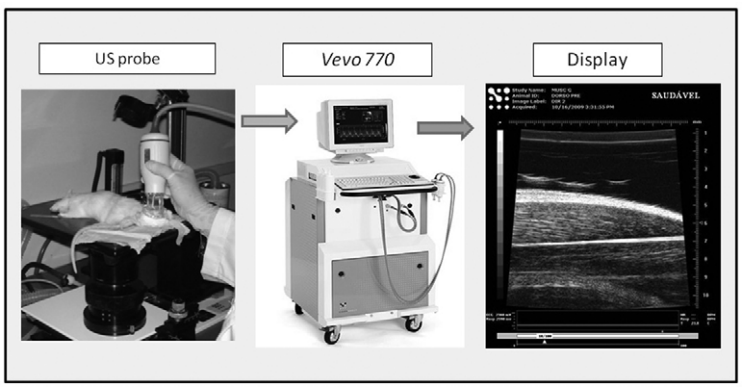

Fig. 1. Experimental setup including the animal laying over a platform and in contact with the ultrasound (US) probe, the ultrasound biomicroscopy (UBM) Vevo 770 equipment and a typical image from the muscles in the leg of the rat *Rattus norvegicus*.

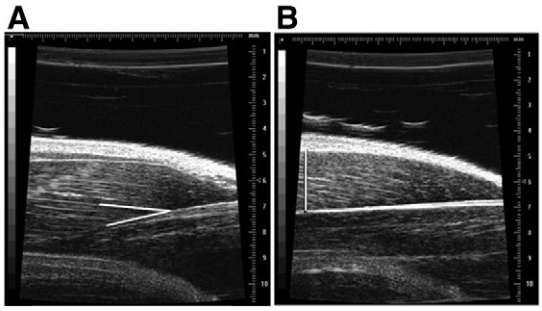

Fig. 2. UBM image showing muscle details and the traces used to quantify (A) pennation angle (PA) and (B) muscle thickness (MT) in *R. norvegicus*.

Quantification of architectural parameters

The PA and MT were measured over the high-resolution ultrasound images obtained from longitudinal planes related to muscle belly at previously identified anatomical points (for MT) or at the more visually distinguishable fibers (for PA). Image processing software (ImageJ, National Institutes of Health, Bethesda, MD, USA) was used to determine the measurements after adjusting gray scale and magnification levels of the images, so that the structures could be well visualized.

MT was calculated as the distance between the superficial and the deep aponeuroses, considering the left side of the ultrasound image. The PA was calculated as the positive angle between the deep aponeurosis and the line of the fascicle (Fig. 2).

For each animal, five good-quality image frames were selected among 100 frames of the videos recorded by the UBM equipment. In each of the five frames, two independent measurements of both parameters were randomly performed, with a total of 10 measures for each rat in each of the ankle positions.

Statistical analysis

Statistical analysis was conducted with the software STATISTICA 7.0 (StatSoft, Tulsa, OK, USA). The normality of data for all groups was tested using the Kolmogorov–Smirnov test. For VG rats, the tests analyzed data dispersion and reliability, and compared the measurement values of two different days of image acquisition as well as values of the different ankle positions. Pearson correlation coefficients were calculated to assess the reliability between two random measurements from the same image for VG rats. For all three groups, coefficients of variation were calculated for both parameters (PA and MT) in all the conditions studied. One-way ANOVA ($P<0.05$) tested the differences among rats for PA and MT. Two-way repeated-measures ANOVAs were used to analyze the differences in PA and MT measured twice in the five selected frames (image × measure); to compare the results obtained on two different days and with the two ankle positions (days × ankle position) for VG rats; and to compare values of different intervals after injury between right and left limbs (interval × limb) for SG and GG rats. One-way ANOVA tested the difference in PA and MT among the four intervals for the control group. *F*-ratios were considered significant at $P<0.05$. Significant differences among means at $P<0.05$ were detected using Tukey's *post hoc* tests.

RESULTS

Images

Images showing the muscle structures with proper definition and distinguishable fascicles, allowing quantification of the selected architectural parameters are presented in Fig. 2. Images showing the LG and the SOL at different intervals before (0 days) and after injury (7, 14, 21 and 28 days) are shown in Figs 3 and 4.

Statistical analysis revealed no differences between all measurements of distinct animals and also no differences between the variables measured twice in each of the five frames. Therefore, the mean values were used for further tests.

VG

Mean ± s.d., coefficient of variation and Pearson correlation values for PA and MT of the LG from VG rats are presented in Table 1. There was no statistical difference between mean values obtained on the two days of testing for each ankle position, assuring test reproducibility and allowing the utilization of all the values for the other statistical tests. A significant increase ($P<0.05$) was observed in both PA and MT at full extension in comparison to the neutral position, demonstrating that both PA and MT change with joint angle (Table 1). Analysis of the coefficients of variation of VG rats showed lower CV values for the full extension position, determining the use of this position for the tests with SG and GG rats.

GG

Mean ± s.d. and coefficient of variation values for PA and MT of the LG from both limbs of GG rats at different moments after injury are presented in Tables 2 and 3. It was not possible to quantify the parameters of the right limb at 7 and 14 days after injury because of changes in the organizational pattern of muscle fibers. Therefore, statistical comparison between two legs was restricted to the following moments: healthy (0 days) and 21 and 28 days after injury.

A progressive and significant increase in PA values of the left limb ($P=0.0001$) was detected, whereas the right limb maintained pre-injury values (Tables 2 and 3). MT values showed a tendency to increase, although a significant difference between the healthy right limb and the left limb was only detected 28 days after injury ($P=0.008$). ANOVA of data from the five intervals (0, 7, 14, 21 and 28 days after injury) of the left limb (non-injured) showed a gradual increase in PA (10.67 to 16.52 deg) and MT (2.92 to 3.13 mm), with statistical differences designated in Table 3.

SG

Mean ± s.d. and coefficient of variation values for PA and MT of the SOL from both limbs of SG rats at different moments before (0 days) and after injury are presented in Tables 4 and 5.

Similarly to the responses detected for GG rats, SG rats showed a gradual increase in PA values for the injured limb during the period of analysis, with a statistically significant difference from the healthy muscle ($P<0.001$) at different intervals after lesion (Table 4). MT showed no significant differences. ANOVA of the two parameters

Table 1. Statistical results for pennation angle (PA) and muscle thickness (MT) for the ankle in neutral position and at full extension for rats in the variability group

	Mean ± s.d.	CV (%)	*r*
Neutral position			
PA (deg)[a]	9.69±1.49	15.41	0.93
MT (mm)[a]	2.79±0.14	4.99	0.99
Full extension			
PA (deg)	16.18±1.52	9.37	0.93
MT (mm)	3.13±0.12	3.97	0.99

CV, coefficient of variation; *r*, Pearson correlation coefficient.
[a]Significant difference to the same parameter at full extension ($P<0.05$).

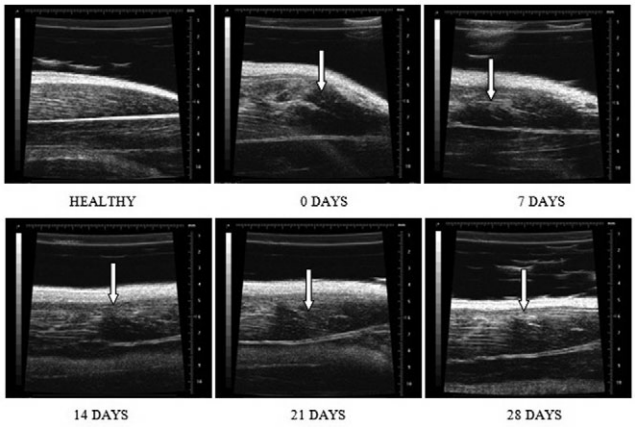

Fig. 3. Sequence of ultrasonic images of the lateral gastrocnemius of the right limb of *R. norvegicus* at the different intervals (before and after injury). Healthy: fascicles and aponeurosis intact, allowing the identification of PA and MT; 0 days (immediately after injury): tissue disorganization and disruption of the fascicles and aponeurosis, with hypoechoic areas representing hemorrhage and edema (arrow), and MT significantly increased; 7 and 14 days: internal aponeurosis reorganized with discontinuation of the fascicles (arrows), which prevents measurements of PA and MT; 21 days: tissue reorganization with a gap (arrow) between the fascicles; 28 days: appearance of hyperechoic bundles (arrow) associated with fibroadipose connective scar tissue.

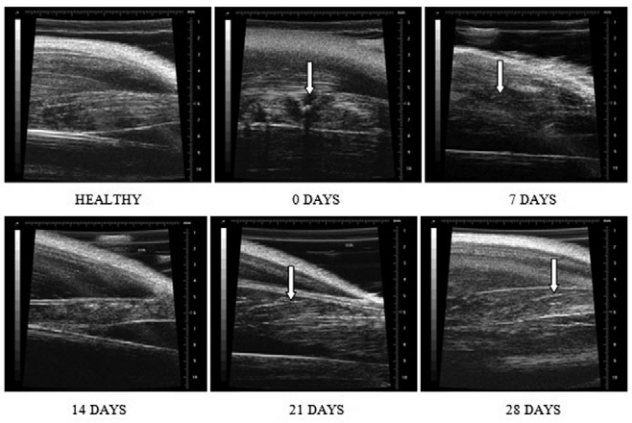

Fig. 4. Sequence of ultrasonic images of the soleus of the right limb of *R. norvegicus* at the different intervals (before and after injury). Healthy: fascicles and aponeurosis intact, allowing the identification of PA and MT; 0 days (immediately after injury): tissue disorganization and disruption of the fascicles and aponeurosis, with hypoechoic areas (arrow) corresponding to hemorrhage and edema; 7 days: disorganized tissue, apparently loose fascicles (arrow) without connection to aponeurosis and discontinuity of superficial aponeurosis; 14 days: internal aponeurosis reorganized with discontinuation of the fascicles, which prevents measurements of PA and MT; 21 and 28 days: appearance of hyperechoic bundles (arrow) associated with fibroadipose connective scar tissue.

of the left limb measured in all intervals before (0 days) and after injury (Table 5) suggests the same tendency of increase observed for LG, although with no statistical differences for MT and with marginal *P*-values for PA (between healthy condition and intervals of 21 and 28 days after injury, P=0.054).

Control group

There were no statistical differences among the four intervals for either one of the parameters (PA and MT) or muscles (LG and SOL), indicating that there was no growth effect on the architecture parameters for rats of that age. Numerical data are shown in Table 6.

DISCUSSION

Although there are no studies with humans that follow up the muscle degeneration–regeneration process, a few have tried to characterize healthy and injured muscles of humans and rabbits with conventional ultrasound equipment of lower frequencies (between 5 and 7.5 MHz). Even though they do not present a controlled methodology, these studies show images similar to those obtained for the rats in this study (Kim et al., 2002; Järvinen et al., 2005; Järvinen et al., 2000; Kullmer et al., 1997; Harcke et al., 1988). The images of the injured muscle tissue acquired 7 and 14 days after injury induction (Figs 3 and 4) show great qualitative differences from those obtained for healthy muscle and are consistent with the literature for ultrasound studies (frequencies 5.0–7.5 MHz) of muscle injuries (Kim et al., 2002; Järvinen et al., 2005; Järvinen et al., 2000; Kullmer et al., 1997; Harcke et al., 1988). For example, there is considerable reduction of the echo signal level in the area previously constituted of muscle tissue, which corresponds to the appearance of hypoechoic areas without distinguishable fiber structures as viewed in the images of healthy muscle. This can be justified by the appearance of hemorrhagic cavity caused by the lesion, hematoma and edema during the muscle regeneration process. In accordance with Peetrons (Peetrons, 2002), responsible for an ultrasound investigation of lesions in humans, the regeneration process leads to a diffuse hypoechogenicity with the displacement of the fascicles that can be viewed in the ultrasound images. Peetrons reports that most serious injuries involving a large number of muscle fibers, as in laceration injuries, will show hypoechoic or even anechoic hematomas, which may remain localized or extend to a larger area along the muscle fascicles (Peetrons, 2002). According to Menetrey et al. (Menetrey et al., 1999), in a torn muscle the injured area is always filled with hematoma, proliferative granular tissue and connective scar tissue, elements that make the repair complex and may inhibit complete regeneration. All of these characteristics can be observed in images taken 7 and 14 days after the injury of both groups in the present study, with subjective variations between animals.

At 21 and 28 days after injury (Figs 3 and 4), it is possible to visualize fibers and fibrous connective tissue, but the muscle is not yet organized as seen in the healthy images. It is suggested that in this period the muscular tissue is passing through the remodeling phase with the appearance of hyperechoic bundles, which may correspond to scar tissue, which provides the wound tissue with the initial strength to withstand the contraction forces applied to it before completion of the repair process (Grounds, 1991; Kullmer et al., 1997; Järvinen et al., 2005; Järvinen et al., 2000). It was impossible to quantify PA and MT at 7 and 14 days after the injury because of disruption of the internal structure of muscle, as seen in Figs 3 and 4, corresponding to hypoechoic or even anechoic hematomas and total disorganization of muscle fiber alignment. Quantification was possible after 21 and 28 days because of a reorganization of the muscle, even though in some cases the muscle was different from the healthy condition because of excessive connective tissue. The qualitative analysis of the sequence of images acquired (Figs 3 and 4) show for that for healthy conditions, fascicles and aponeurosis are intact, allowing the identification of PA and MT, whereas immediately after the injury there is tissue disorganization and disruption of the fascicles and aponeurosis, with hypoechoic areas representing hemorrhage and edema and MT significantly increased. Seven and 14 days after the injury, the internal aponeurosis is

Table 2. Statistical results for PA and MT of the right limb (injured) of rats in the gastrocnemius injured group (GG)

	Interval (days)	Mean ± s.d. (deg)	CV (%)
PA	0	10.99±0.81	7.38
	21	10.95±0.62	5.66
	28	10.83±0.92	8.5
	Interval (days)	Mean ± s.d. (mm)	CV (%)
MT	0	2.69±0.34	12.57
	21	2.83±0.2	6.93
	28	2.85±0.13	4.68

Table 3. Statistical results for PA and MT of the left limb (non-injured) of GG rats

	Interval (days)	Mean ± s.d. (deg)	CV (%)
PA	0	10.68±1.19	11.13
	7	12.65±1.16	9.13
	14[a]	15.25±1.89	12.38
	21[a]	13.79±1.47	10.63
	28[a,b]	16.53±1.85	11.19
	Interval (days)	Mean ± s.d. (mm)	CV (%)
MT	0	2.92±0.16	5.5
	7	2.94±0.22	7.49
	14	2.88±0.14	4.88
	21	2.93±0.06	1.97
	28	3.13±0.2	6.4

[a]Significant difference to 0 days after injury (P<0.05).
[b]Significant difference to 7 days after injury (P<0.05).

Table 4. Statistical results for PA and MT of the right limb (injured) of rats in the soleus injured group (SG)

	Interval (days)	Mean ± s.d. (deg)	CV (%)
PA	0	8.22±2.45	29.89
	21[a]	10.92±2.47	22.6
	28[a]	7.64±3.87	50.73
	Interval (days)	Mean ± s.d. (mm)	CV (%)
MT	0	2.25±0.27	12.34
	21	2.075±0.305	14.71
	28	2.082±0.48	23.14

[a]Significant difference to left limb in the same interval after injury (P<0.05).

Table 5. Statistical results for PA and MT of the left limb (non-injured) of SG rats

	Interval (days)	Mean ± s.d. (deg)	CV (%)
PA	0	9.65±0.96	9.95
	7	12.04±2.03	16.9
	14[a]	11.15±4.045	36.26
	21[a]	14.1±1.4	9.96
	28[a,b]	14.06±2.29	16.28
	Interval (days)	Mean ± s.d. (mm)	CV (%)
MT	0	2.12±0.23	10.94
	7	2.14±0.36	16.99
	14	2.4±0.25	10.8
	21	1.87±0.42	22.85
	28	2.35±0.46	19.52

[a]Significant difference to healthy condition (P<0.05).
[b]Significant difference to 7 days after injury (P<0.05).

reorganized although there is discontinuation of the fascicles, which prevents measurements of PA and MT. Twenty-one days after the laceration the tissue reorganization can be visualized, with occasional gaps between the fascicles, and 28 days after the injury it is possible to detect the appearance of hyperechoic bundles associated with fibroadipose connective scar tissue.

The PA of the left limb (non-injured) in GG rats increased from 10.68 to 16.53 deg, which corresponds to an increase of 54.77%, much higher than the coefficient of variation of PA obtained in the variability study of this measure. So, it is possible that there is a significant increase (both statistically and physiologically) in PA of the healthy limb during the muscle regeneration of the contralateral limb. The same can be observed for the variation in the PA in SG rats, with a percentage increase of 45.69% (9.65 to 14.06 deg). MT of the GG and SG rats ranged from 2.92 to 3.13 mm (7.56%) and 2.12 to 2.35 mm (10.84%), respectively, values well above the coefficient of variation for MT of VG rats (3.97%). Significant variation of the parameters during a period of 28 days was not observed for the control group, indicating that the increase in PA in the GG and SG rats cannot be attributed to muscle normal growth.

The gradual increase in the PA and trend of increase of the MT of the left limb (non-injured) observed in this study suggest a compensatory hypertrophic response of the healthy contralateral limb, which was subjected to increased load during the period in which the force production by the injured limb could provoke a rerupture of muscle tissue. As described in classic literature on muscle biomechanics, for a known physiological cross-sectional area and a known volume, an increased PA can, in many cases, result in a reduction of fiber length, compromising the velocity of shortening and the amplitude of variation of length, but it also allows a greater amount of contractile material to be arranged in parallel, increasing the capacity of force and maximum force (Gans, 1982; Lieber, 2002).

Studies with humans that investigated the changes in muscle architecture caused by strength training showed that muscle fibers hypertrophy in response to the training and, consequently, increase in size (Blazevich, 2006; Blazevich et al., 2007; Boonyarom and Inui, 2006; Kawakami, 2005). These studies measured muscle size using indirect estimates of MT. In relation to the PA, the literature suggests that there are intermuscular differences in responses induced by training on fiber architecture. Nevertheless, the increase in PA is a common consequence of pennate hypertrophied muscles (Kawakami, 2005; Blazevich, 2006; Narici and Cerretelli, 1998; Kawakami et al., 1993).

Narici and Cerretelli detected lower values of anatomical cross-sectional area (23.1±2.8%), fiber length (12.7±1.9%) and PA (16.42±2.9%) for the injured medial gastrocnemius of humans with unilateral atrophy when compared with healthy subjects (Narici and Cerretelli, 1998). These results are similar to those presented in this study. Although their study was performed with humans with a different type of lesion, biomechanical characteristics were affected by conditions of reduced overload and dysfunction. Nevertheless, our results indicate that the differences between limbs (injured *versus* non-injured) are due to an increase in the healthy limb parameters instead of a reduction in the corresponding parameters of the injured limb.

Studies with animals normally use histological analyses and *in vitro* techniques to assess muscle under different conditions. Filho et al. (Filho et al., 2006) studied the response of the muscle fibers of the SOL of rats subjected to exercise on a treadmill through

Table 6. Statistical results for PA and MT of rats in the control group

	PA			MT		
Muscle	Interval (days)	Mean ± s.d. (deg)	CV (%)	Interval (days)	Mean ± s.d. (mm)	CV (%)
LG	0	13.45±2.02	15.01	0	3.23±0.28	8.67
	7	12.54±1.18	9.4	7	3.14±0.22	7.01
	21	12.53±1.26	10.05	21	3.31±0.2	6.04
	28	12.28±1.62	13.19	28	3.28±0.34	10.37
SOL	0	6.05±1.38	22.84	0	1.38±0.18	12.76
	7	6.22±1.34	21.49	7	1.37±0.14	10.29
	21	5.99±1.04	17.42	21	1.35±0.18	13.31
	28	6.14±1.51	24.62	28	1.33±0.19	14.56

LG, lateral gastrocnemius; SOL, soleus.

histology and reported significant increases in the diameters of fibers. Moreover, these authors detected by histological and histochemical analysis events such as polymorphism, as well as angular atrophic fibers, rounded fibers, increased enzymatic activity in some fibers and an almost total absence of activity in others, suggesting muscle hypertrophy, although this was dependent on the application time of exercise. These results also indicate a compensatory hypertrophic response in the healthy overloaded limb, and are in accordance with our findings.

In a recent study, Eng et al. examined muscle architectural properties of the rat hindlimb through *in vitro* techniques to examine each muscle's functional specialization (Eng et al., 2008). The authors measured surface PA with a standard goniometer after dissecting the specimens with the hip and knee held at 90 deg and the ankle in neutral position, and found values of 14.2±3.6 deg for the LG. Differences for the results obtained *in vivo* in the present study may be explained by the different technique approaches (*in vivo* and *in vitro*): rigor mortis state, which provokes a slow contraction of muscle fibers; connective tissue contraction and/or muscle length reduction because of the fixation process; and position at which muscles are fixed (Martin et al., 2001). Eng et al. (Eng et al., 2008) fixed the muscles with the ankle in neutral position and with different positions of knee and hip, and it has been reported that positioning of involved joints modifies the PA (Abellaneda et al., 2009; Maganaris et al., 1998; Narici, 1999).

Strict methodologies were used in the present study in order to minimize measurement errors: all images were double-digitized, all digitizing was undertaken by a single operator and the UBM machine was always operated by the same individual to remove multiple-operator unreliability. The measurements in the present study had a coefficient of variation of 9.37 and 3.97% for PA and MT, respectively, for the ankle at full extension and 15.41 and 4.99% for the ankle at neutral position. These results are lower than those reported in studies with humans. Blazevich et al. reported coefficients of variation of approximately 15–20% and 30–40% for similar procedures of measuring PA and MT, respectively of human vastus lateralis with conventional ultrasound imaging (Blazevich et al., 2007). Ito et al. reported a coefficient of variation of 7% for PA of human tibialis anterior (Ito et al., 1998).

Studies in humans have shown that MT and PA are highly correlated with the joint positioning. Maganaris et al. (Maganaris et al., 1998) and Narici et al. (Narici et al., 1996) reported that medial gastrocnemius architecture is significantly affected by changes in joint angle both at rest and at maximum voluntary contraction. In the present study, this relationship was confirmed for rats by an increase in PA from 9.69±1.49 to 16.17±1.52 deg (P<0.05) and an increase in MT from 2.79±0.14 to 3.13±0.12 mm (P<0.05) for ankle joint angles varying from 104.86±3.13 to 151.8±2.60 deg, respectively. Nevertheless, further research with a larger sample is needed to fully analyze the correlative relationship of this data. Analysis of these results determined the utilization of the position of full extension for further tests with the SG and GG rats. Variability of the ankle angle in this position was analyzed in terms of the coefficient of variation of measurements made at intervals of 14, 21 and 28 days of GG rats (4.35, 3.54 and 4.12%, respectively). The variation was considered too small to influence the values of PA obtained.

Some limitations of the present study should be considered. The injury protocol was not strictly controlled; although it was performed as described in the literature and by the same researcher, differences in the characteristics of the lesion (size, position, depth) remained between rats. Moreover, an improved and controlled methodology of limb positioning and ankle angle determination is suggested to assure minimal variations of muscle geometry associated with varying muscular positions.

Knowledge of muscle architectural response and geometric adaptations of muscle fascicles can influence and establish directions for rehabilitation and athletic programs, as well as improve mathematical models that predict performance and changes in muscle force that follow interventions of training and detraining. Comparative studies of muscle architecture in healthy conditions and after different types of injury or disorder are of great importance, and the UBM technique has shown its potential as a tool for such research on animal models.

Conclusions

Reliability of PA and MT measurements with UBM was high for repeated image acquisition and digitization for the proposed methodology. The coefficient of variation for all measurements indicates good procedural reproducibility.

The PA and MT of the LG change with ankle angle, although we suggest that this position should be strictly controlled in future triceps surae muscle architecture studies in rats.

The increase in the PA of the left limb (non-injured) in GG (10.68 to 16.53 deg, 54.77%) and SG rats (9.65 to 14.06 deg, 45.69%), along with the variation in MT of GG (2.92 to 3.13 mm, 7.56%) and SG rats (2.12 to 2.35 mm, 10.84%), suggests that there is a compensatory hypertrophic response of the contralateral healthy limb because of the overloaded condition imposed during the period in which the force production by the injured limb could provoke a rerupture of muscle tissue.

So far, studies of skeletal muslce injuries in humans have not allowed evaluation prior to injury. This is possible in animal studies using the UBM technique, the potential application for analysis of skeletal muscle tissue of which was studied in this work.

LIST OF ABBREVIATIONS

GG	gastrocnemius injured group
LG	lateral gastrocnemius
MT	muscle thickness
PA	pennation angle
SG	soleus injured group
SOL	soleus
UBM	ultrasound biomicroscopy
VG	variability group

ACKNOWLEDGEMENTS

The authors are thankful for the financial support provided by CAPES/PROEX, CNPq and FAPERJ; for the collaboration of the Biophysics Institute, through the Antonio Paes de Carvalho Laboratory, allowing the use of the UBM system; and for the collaboration of the Exercise and Muscular Biology Laboratory, which provided the animals for the research.

REFERENCES

Abellaneda, S., Guissard, N. and Duchateau, J. (2009). The relative lengthening of the myotendinous structures in the medial gastrocnemius during passive stretching differs among individuals. *J. Appl. Physiol.* **106**, 169-177.

Blazevich, A. J. (2006). Effects of physical training and detraining, immobilisation, growth and aging on human fascicle geometry. *Sports Med.* **36**, 1003-1017.

Blazevich, A. J., Gill, N. D., Deans, N. and Zhou, S. (2007). Lack of human muscle architectural adaptation after short-term strength training. *Muscle Nerve* **35**, 78-86.

Boonyarom, O. and Inui, K. (2006). Atrophy and hypertrophy of skeletal muscles: structural and functional aspects. *Acta Physiol.* **188**, 77-89.

Eng, C. M., Smallwood, L. H., Rainiero, M. P., Lahey, M., Ward, S. R. and Lieber, R. L. (2008). Scaling of muscle architecture and fiber types in the rat hindlimb. *J. Exp. Biol.* **211**, 2336-2345.

Filho, J. C. S. C., Vanderlei, L. C. M., Camargo, R. C. T., Oliveira, D. A. R., Junior, S. A. O., Dal Pai, V. and Belangero, W. D. (2006). Análise histológica, histoquímica e morfométrica do músculo sóleo de ratos submetidos a treinamento físico em esteira rolante. *Arq. Ciênc. Saúde* **12**, 196-199.

Foster, F. S. (2003). *In vivo* imaging of embryonic development in the mouse eye by ultrasound biomicroscopy. *Invest. Ophthalmol. Vis. Sci.* **44**, 2361-2366.

Foster, F. S., Zhang, M. Y., Zhou, Y. Q., Liu, G., Mehi, J., Cherin, E., Harasiewicz, K. A., Starkoski, B. G., Zan, L., Knapik, D. A. et al. (2002). A new ultrasound instrument for *in vivo* microimaging of mice. *Ultrasound Med. Biol.* **28**, 1165-1172.

Fukunaga, T., Kawakami, Y., Kuno, S., Funato, K. and Fukashiro, S. (1997). Muscle architecture and function in humans. *J. Biomech.* **30**, 457-463.

Gans, C. (1982). Fibre architecture and muscle function. *Exerc. Sport Sci. Rev.* **10**, 160-207.

Grounds, M. D. (1991). Towards understanding skeletal muscle regeneration. *Pathol. Res. Pract.* **187**, 1-22.

Harcke, H. T., Grissom, L. E. and Finkelstein, M. S. (1988). Evaluation of the musculoskeletal system with sonography. *AJR Am. J. Roentgenol.* **150**, 1253-1261.

Hashimoto, B. E., Kramer, D. J. and Wiitala, L. (1999). Applications of musculoskeletal sonography. *J. Clin. Ultrasound* **27**, 293-318.

Ito, M., Kawakami, Y., Ichinose, Y., Fukashiro, S. and Fukunaga, T. (1998). Nonisometric behavior of fascicles during isometric contractions of a human muscle. *J. Appl. Physiol.* **85**, 1230-1235.

Jacobson, J. A. (1999). Musculoskeletal sonography and MR imaging a role for both imaging methods. *Radiol. Clin. North Am.* **37**, 713-735.

Järvinen, T. A. H., Kääriäinen, M., Järvinen, M. and Kalimo, H. (2000). Muscle strain injuries. *Curr. Opin. Rheumatol.* **12**, 155-161.

Järvinen, T. A. H., Järvinen, T. L. N., Kääriäinen, M., Kalimo, H. and Järvinen, M. (2005). Muscle injuries: biology and treatment. *Am. J. Sports Med.* **33**, 745-764.

Kawakami, Y. (2005). The effects of strength training on muscle architecture in humans. *Int. J. Sport Health Sci.* **3**, 208-217.

Kawakami, Y., Abe, T. and Fukunaga, T. (1993). Muscle fiber pennation angles are greater in hypertrophied than in normal muscles. *J. Appl. Physiol.* **74**, 2740-2744.

Kawakami, Y., Ichinose, Y. and Fukunaga, T. (1998). Architectural and functional features of human triceps surae muscles during contraction. *J. Appl. Physiol.* **85**, 398-404.

Kim, H. J., Ryu, K. N., Shung, D. W. and Park, Y. K. (2002). Correlation between sonographic and pathologic findings in muscle injury: experimental study in the rabbit. *J. Ultrasound Med.* **21**, 1113-1119.

Koryak, Y. A. (2008). Functional and clinical significance of the architecture of human skeletal muscles. *Hum. Physiol.* **34**, 482-492.

Kullmer, K., Sievers, K. W., Rompe, J. D., Nagele, M. and Harland, U. (1997). Sonography and MRI of experimental muscle injuries. *Arch. Orthop. Trauma Surg.* **116**, 357-361.

Lieber, R. L. (2002). *Skeletal Muscle Structure, Function & Plasticity – The Physiological Basis of Rehabilitation*, 2nd edn. Philadelphia, PA: Lippincott Williams & Wilkins.

Lieber, R. L. and Bodine-Fowler, S. C. (1993). Skeletal muscle mechanics: implications for rehabilitation. *Phys. Ther.* **73**, 844-856.

Maganaris, C. N., Baltzopoulos, V. and Sargeant, A. J. (1998). *In vivo* measurements of the triceps surae complex architecture in man: implications for muscle function. *J. Physiol.* **512**, 603-614.

Martin, D. C., Medri, M. K., Chow, R. S., Oxorn, V., Leekam, R. N., Agur, A. M. and McKee, N. H. (2001). Comparing human skeletal muscle architectural parameters of cadavers with *in vivo* ultrasonographic measurements. *J. Anat.* **199**, 429-434.

Megliola, A., Eutropi, F., Scorzelli, A., Gambacorta, D., De Marchi, A., De Filippo, M., Faletti, C. and Ferrari, F. S. (2006). Ultrasound and magnetic resonance imaging in sports-related muscle injuries. *Radiol. Med.* **111**, 836-845.

Menetrey, J., Kasemkijwattana, C., Fu, F. H., Moreland, M. S. and Huard, J. (1999). Suturing versus immobilization of a muscle laceration. *Am. J. Sports Med.* **27**, 222-229.

Narici, M. (1999). Human skeletal muscle architecture studied *in vivo* by non-invasive imaging techniques: functional significance and applications. *J. Electromyogr. Kinesiol.* **9**, 97-103.

Narici, M. and Cerretelli, P. (1998). Changes in human muscle architecture in disuse-atrophy evaluated by ultrasound imaging. *J. Gravit. Physiol.* **5**, 73-74.

Narici, M. V., Binzoni, T., Hiltbrand, E., Fasel, J., Terrier, F. and Cerretilli, P. (1996). *In vivo* human gastrocnemius architecture with changing joint angle at rest and during graded isometric contraction. *J. Physiol.* **496**, 287-297.

Peetrons, P. (2002). Ultrasound of muscles. *Eur. Radiol.* **12**, 35-43.

Ward, S. R., Eng, C. M., Smallwood, L. H. and Lieber, R. L. (2009). Are current measurements of lower extremity muscle architecture accurate?. *Clin. Orthop. Relat. Res.* **467**, 1074-1082.

Wickiewicz, T. L., Roy, R. R., Powell, P. L. and Edgerton, V. R. (1983). Muscle architecture of the human lower limb. *Clin. Orthop. Relat. Res.* **179**, 275-283.

Witte, R. S., Dow, D. E., Olafsson, R., Shi, Y. and O'Donnell, M. (2004). High resolution ultrasound imaging of skeletal muscle dynamics and effects of fatigue. In *IEEE International Ultrasonics, Ferroelectrics, and Frequency Control Joint 50th Anniversary Conference Proceedings*, pp. 764-767. Montréal: IEEE Ultrasonics Symposium.